

---

**MAJOR PAPER**

---

**Hepatic Relaxation Times from Postmortem MR Imaging of Adult Humans**Seiji SHIOTANI<sup>1\*</sup>, Tomoya KOBAYASHI<sup>2</sup>, Hideyuki HAYAKAWA<sup>3</sup>, Kazuhiro HOMMA<sup>4</sup>,  
and Harumi SAKAHARA<sup>5</sup><sup>1</sup>*Department of Radiology, Seirei Fuji Hospital  
3-1 Minami-cho, Fuji, Shizuoka 417-0026, Japan*<sup>2</sup>*Department of Radiological Technology, Tsukuba Medical Center Hospital*<sup>3</sup>*Department of Forensic Medicine, Tsukuba Medical Examiner's Office*<sup>4</sup>*Evaluation Department, National Institute of Advanced Industrial Science and Technology*<sup>5</sup>*Department of Radiology, Hamamatsu University School of Medicine*

(Received March 28, 2015; Accepted October 28, 2015; published online December 22, 2015)

**Purpose:** To measure  $T_1$  and  $T_2$  values of hepatic postmortem magnetic resonance (PMMR) imaging.

**Materials and Methods:** We performed hepatic PMMR imaging of 22 deceased adults (16 men, 6 women; mean age, 56.3 years) whose deaths were for reasons other than liver injury or disease at a mean of 27.7 hours after death. Before imaging, the bodies were kept in cold storage at 4°C (mean rectal temperature, 17.6°C). We measured  $T_1$  and  $T_2$  values in the liver at two sites (the anterior segment of the right lobe and the lateral segment of the left lobe). We also investigated the influence of the body temperature and postmortem interval on  $T_1$  and  $T_2$  values.

**Results:** In the anterior segment of the right lobe and the lateral segment of the left lobe,  $T_1$  values of PMMR imaging were  $524 \pm 112$  ms and  $472 \pm 104$  ms (mean  $\pm$  standard deviation), respectively; while  $T_2$  values were  $42 \pm 6$  ms and  $43 \pm 8$  ms, respectively.  $T_1$  and  $T_2$  values did not differ significantly between the two sites ( $P \geq 0.05$ ). Regarding temperature, the  $T_2$  values of hepatic PMMR imaging were linearly correlated with the body temperature, but the  $T_1$  values were not. The  $T_1$  and  $T_2$  values of the two sites in the liver did not correlate with the postmortem interval.

**Conclusion:** Reduction in body temperature after death is considered to induce  $T_1$  and  $T_2$  value changes in the liver on PMMR imaging.

**Keywords:** *liver, in vivo, low body temperature,  $T_1$  and  $T_2$  values, postmortem magnetic resonance imaging*

**Introduction**

While the worldwide decline in the rate of conventional autopsies has increased the need for and frequency of postmortem imaging as a complementary, supplementary, or alternative method of autopsy,<sup>1–8</sup> there continues to be insufficient postmortem imaging data for some parts of the human body due to lack of data obtained at various imaging settings.

Postmortem magnetic resonance (PMMR) imaging can provide more detailed information with better contrast resolution than postmortem computed tomography (PMCT), and depict some pathological conditions that are difficult to identify with PMCT.<sup>9</sup> However, PMMR imaging has revealed that both MR signals and image contrast change after death, which can deteriorate diagnostic accuracy.<sup>9–13</sup> The optimization of parameters for PMMR imaging and accurate interpretation of imaging findings require analyses of quantitative data.<sup>14–16</sup>  $T_1$  and  $T_2$  values on MR imaging of the human adult liver *in vitro* and *in vivo* have been reported.<sup>17–22</sup> We surmised that the quantitative data of  $T_1$  and  $T_2$  values of hepatic PMMR imaging of *in vivo* would help interpret postmortem imaging variation relative to

---

\*Corresponding author, Phone: +81-545-52-0780, Fax: +81-545-52-0813, E-mail: s.shiotani@sis.seirei.or.jp

©2015 Japanese Society for Magnetic Resonance in Medicine  
This work is licensed under a Creative Commons Attribution-NonCommercial-NoDerivatives International License.

postmortem interval (time elapsed after death), functional failure before death, and/or metabolic abnormality resulting from pharmacologic or toxic substances. A newly published first-impression postmortem study using a 3.0T scanner reported that different magnetic field strengths, such as 1.5T, would result in different quantitative values for  $T_1$  and  $T_2$  for the same tissue and temperature.<sup>16</sup> We report the  $T_1$  and  $T_2$  values of 1.5T PMMR imaging of an adult human liver *in vivo*.

## Materials and Methods

### Subjects

We examined PMMR imaging data of 22 adults (16 men, 6 women; aged 27–83 years, mean: 56.3 years) who died suddenly and unexpectedly and did not have abnormal results nor indications of fatty liver on hepatopathological examination. Both ascites around the liver and putrefaction gas formation were ruled out using whole-body PMCT immediately before PMMR imaging. Their bodies were kept in cold storage at 4°C and subjected to PMMR imaging 7 to 96 hours after the confirmation of death (mean: 27.7 hours). Their rectal temperatures, measured immediately after PMMR imaging with an industrial thermometer (7-257-01, AS ONE Corp., Osaka, Japan), were 5–31°C (mean: 17.6°C).

Autopsy was performed on each subject after PMMR imaging. Causes of death were 5 cases of trauma not involving the abdomen (cervical injuries due to road traffic accidents), 5 cases of ischemic heart disease (coronary arterial thrombus and/or myocardial infarction), 5 cases of acute heart failure due to fatal arrhythmia, 3 cases of drowning in the bathtub, 2 cases of cerebral hemorrhage, and 1 case each of subarachnoid hemorrhage and acute drug intoxication.

### Scan conditions

With the permission of our institutional ethics committee, we performed PMMR imaging using a 1.5T MR imaging clinical scanner (Avanto, Siemens, Erlangen, Germany) with a dedicated 6-channel body matrix coil and spine matrix coil. We measured  $T_1$  and  $T_2$  values with a relaxation time map creation tool (syngo MapIt, Siemens, Erlangen, Germany).<sup>23</sup> Table 1 shows the scan parameters for the liver. A dual-flip angle technique based on the 3D-FLASH spoiled gradient echo sequence was employed for  $T_1$  mapping.  $T_2$  mapping was based on a multi-echo spin echo sequence. However, the first echo was ignored in the pixel-wise calculation of the  $T_2$  map, since it consistently yielded a lower signal than the second echo. Inhomogeneity correction was performed for static magnetic field ( $B_0$ ); however, it was not performed for radiofrequency magnetic field ( $B_1$ ).

**Table 1.** Scan parameters of postmortem magnetic resonance (PMMR) imaging based on the syngo MapIt method

Scan parameters	$T_1$ map (GE)	$T_2$ map (SE)
TR/TE (ms)	15/1.62	2000/30, 60, 90, 120, 150
Flip angle	5°, 26°	180°
Slice thickness/gap (mm)	3/0	5/1
Matrix size (mm)	1.2 × 1.2	1.2 × 1.2
Field of view (FOV) (mm)	300	300
Scan time (min)	2.1	3.6
Number of slices	22 (3D)	11

GE, gradient echo; SE, spin echo; TR, repetition time; TE, echo time; 3D, three-dimensional

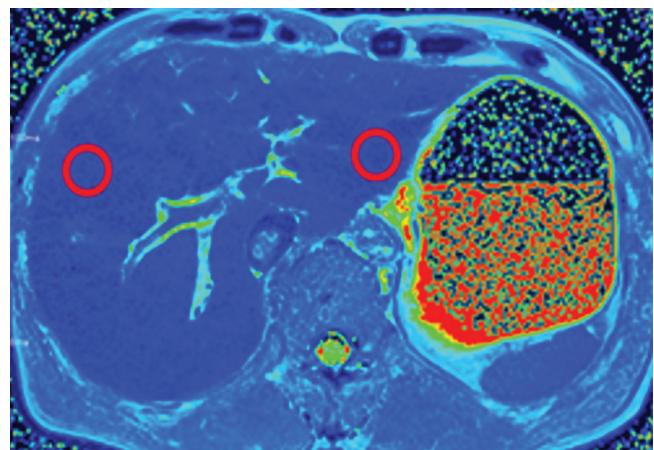


**Fig. 1.** Postmortem 1.5T magnetic resonance (MR) image of the liver. Red circles indicate regions of interest (ROIs) placed at the level of the main trunk of the portal vein on postmortem MR images. ROIs were placed on the anterior segment of the right lobe and lateral segment of the left lobe.

### Analyses

A radiological technologist (T.K.) with 16 years of experience defined 2-cm-diameter circular regions of interest (ROIs) in the liver in both the anterior segment of the right lobe and the lateral segment of the left lobe excluding the vessels and bile ducts on axial images at the level of the main trunk of the portal vein (Fig. 1).

Statistical analyses were performed using statistical software (Excel 2010, Microsoft, Redmond, WA, USA) with Statcel 2 (OMS, Tokyo, Japan) an add-in software. Parametric statistics (arithmetic mean value ± standard deviation [SD]) and Student's t-test were used with a significance value of  $P < 0.05$  for group differences.

The relationships among  $T_1$  values,  $T_2$  values, and rectal temperatures were analyzed with Pearson's correlation coefficient using the least squares methods. Also, the relationships among  $T_1$  values,  $T_2$  values, and postmortem intervals were analyzed using the same methods.

**Results**

A diagnostic radiologist (S.S.) with 24 years of experience observed no specific abnormality, except for signal intensity and contrast, between PMMR imaging (Fig. 2a–d) and clinical MR imaging of the liver. The  $T_1$  values of the anterior segment of the right lobe and the lateral segment of the left lobe were  $524 \pm 112$  ms and  $472 \pm 104$  ms (means  $\pm$  SD), respectively (Table 2),

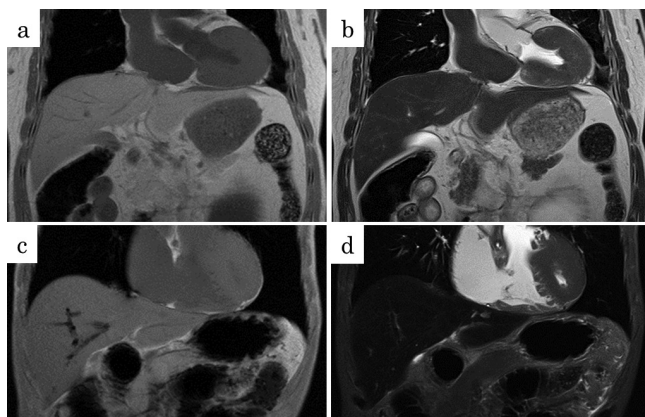


**Fig. 2.** (a) Coronal  $T_1$ -weighted image of the liver on post-mortem magnetic resonance imaging (MRI).  $T_1$  value of the anterior segment of the right lobe and lateral segment of the left lobe is 474.3 and 571.9 ms (rectal temperature: 27.5°C). (b) Coronal  $T_2$ -weighted image of the liver on postmortem MRI.  $T_1$  value of the anterior segment of the right lobe and lateral segment of the left lobe is 57.7 and 54.0 ms (rectal temperature: 27.5°C). (c) Coronal  $T_1$ -weighted image of the liver on postmortem MRI.  $T_2$  value of the anterior segment of the right lobe and lateral segment of the left lobe is 500.5 and 401.5 ms (rectal temperature: 5.0°C). (d) Coronal  $T_2$ -weighted image of the liver on postmortem MRI.  $T_2$  value of the anterior segment of the right lobe and lateral segment of the left lobe is 29.9 and 26.8 ms (rectal temperature: 5.0°C).

**Table 2.**  $T_1$  and  $T_2$  values (ms) in the anterior segment of the right lobe and the lateral segment of the left lobe on hepatic postmortem magnetic resonance imaging

	$T_1$ value (ms)	$T_2$ value (ms)
Anterior segment of the right lobe	$524 \pm 112$	$42 \pm 6$
Lateral segment of the left lobe	$472 \pm 104$	$43 \pm 8$

No significant difference is found between the two sites. ( $T_1$ :  $P = 0.123$ ,  $T_2$ :  $P = 0.823$ ).

showing no significant difference between the two sites ( $P = 0.123$ ,  $t = 1.575 < 2.018 = t_{0.05(42)}$ ). The  $T_2$  values of the anterior segment of the right lobe and the lateral segment of the left lobe were  $42 \pm 6$  ms and  $43 \pm 8$  ms, respectively (Table 2), showing no significant difference between the two sites ( $P = 0.823$ ,  $t = 0.225 < 2.018 = t_{0.05(42)}$ ).

Regarding rectal temperature, with hepatic PMMR imaging,  $T_1$  values of the anterior segment of the right lobe did not correlate significantly with the temperature (correlation coefficient  $r = 0.23$ ;  $P > 0.05$ , Fig. 3); nor did  $T_1$  values of the lateral segment of the left lobe correlate significantly with the temperatures ( $r = 0.13$ ;  $P > 0.05$ , Fig. 4). In contrast,  $T_2$  values of the anterior segment of the right lobe ( $r = 0.45$ ;  $P < 0.05$ , Fig. 5) and  $T_2$  values of the lateral segment of the left

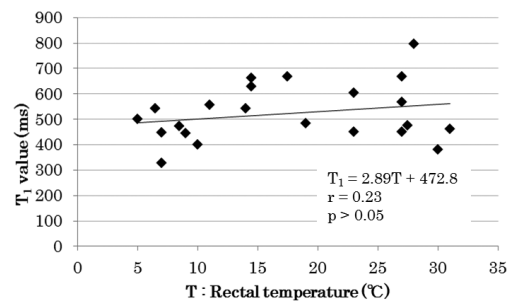


**Fig. 3.** Relationship between  $T_1$  values of the anterior segment of the right lobe and rectal temperature of deceased subjects.

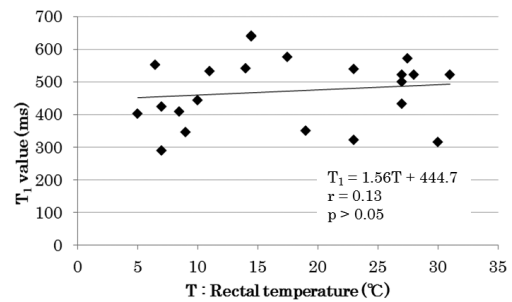


**Fig. 4.** Relationship between  $T_1$  values of the lateral segment of the left lobe and rectal temperature of deceased subjects.

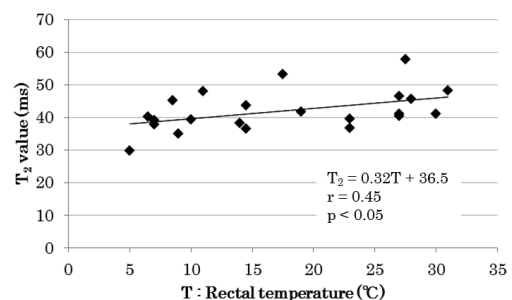


**Fig. 5.** Relationship between  $T_2$  values of the anterior segment of the right lobe and rectal temperature of deceased subjects.

lobe ( $r = 0.52$ ;  $P < 0.05$ , Fig. 6) significantly correlated with the rectal temperature.

Regarding postmortem interval, with hepatic PMMR imaging,  $T_1$  values of the anterior segment of the right lobe (correlation coefficient  $r = -0.26$ ;  $P > 0.05$ , Fig. 7) and  $T_1$  values of the lateral segment of the left lobe ( $r = -0.28$ ;  $P > 0.05$ , Fig. 8) did not correlate significantly with the postmortem interval. Also,  $T_2$  values of the anterior segment of the right lobe ( $r = -0.29$ ;  $P > 0.05$ , Fig. 9) and  $T_2$  values of the lateral segment of the left lobe ( $r = -0.38$ ;  $P > 0.05$ , Fig. 10) did not correlate significantly with the postmortem interval.

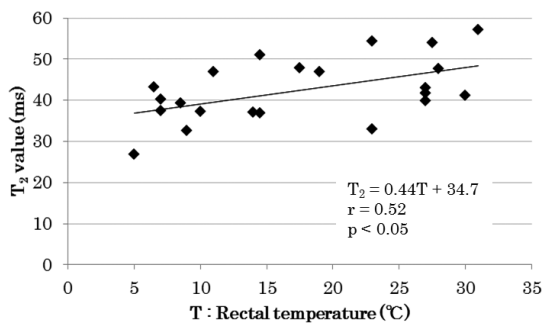


**Fig. 6.** Relationship between  $T_2$  values of the lateral segment of the left lobe and rectal temperature of deceased subjects.

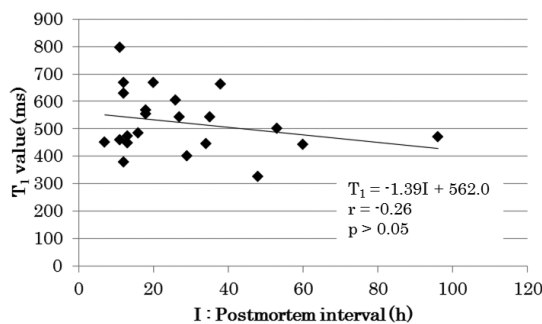


**Fig. 7.** Relationship between  $T_1$  values of the anterior segment of the right lobe and postmortem interval of deceased subjects.

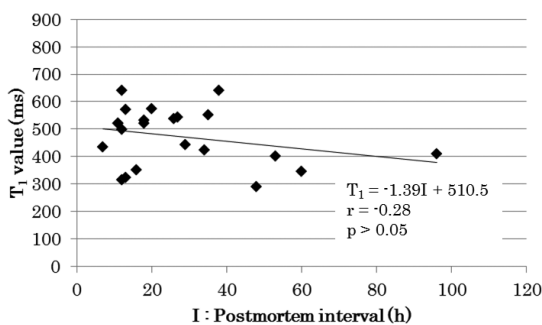


**Fig. 8.** Relationship between  $T_1$  values of the lateral segment of the left lobe and postmortem interval of deceased subjects.

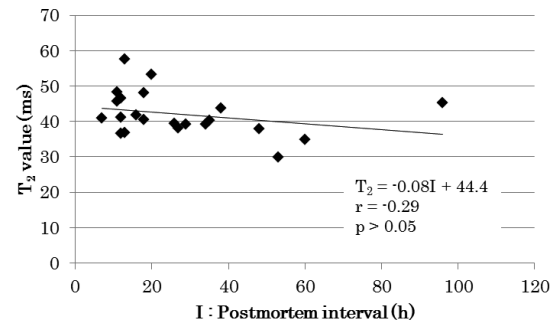


**Fig. 9.** Relationship between  $T_2$  values of the anterior segment of the right lobe and postmortem interval of deceased subjects.

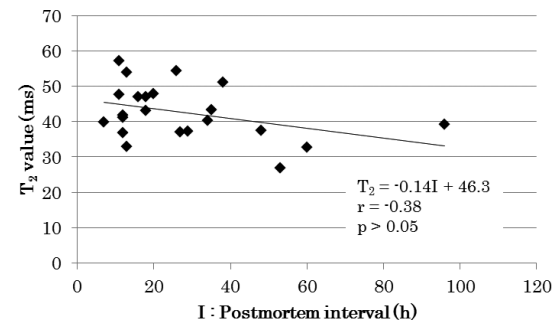


**Fig. 10.** Relationship between  $T_2$  values of the lateral segment of the left lobe and postmortem interval of deceased subjects.

## Discussion

In the present study, the average  $T_1$  values of the anterior segment of the right lobe and the lateral segment of the left lobe on hepatic PMMR imaging at 1.5T were  $524 \pm 112$  ms and  $472 \pm 104$  ms, respectively. The average  $T_2$  values of those two sites were  $42 \pm 6$  ms and  $43 \pm 8$  ms, respectively.  $T_2$  values of the two sites linearly correlated with the body temperature, but  $T_1$  values did not.  $T_1$  and  $T_2$  values of the two sites did not correlate with the postmortem interval.

Zech et al. reported  $T_1$  and  $T_2$  values of hepatic PMMR imaging at 3.0T were 680 and 37 ms.<sup>16</sup> De Bazelaire et al. reported that  $T_1$  values were generally higher and  $T_2$  values were generally lower at 3.0T than at 1.5T in the clinical MR imaging,<sup>22</sup> which agree with the results of our study and those of Zech et al. In the report of de Bazelaire et al., four healthy adult volunteers underwent MR imaging with a whole-body 1.5T MR scanner with a receive-only surface coil array, and  $T_1$  and  $T_2$  values of the liver were measured using an inversion-recovery method with different inversion times and a multiple spin-echo technique with different echo times.<sup>22</sup> Average  $T_1$  and  $T_2$  values of their living subjects' livers were  $586 \pm 39$  ms and  $46 \pm 6$  ms, respectively. Comparing measured  $T_1$  and  $T_2$  values between our deceased subjects and living subjects in the report

of de Bazelaire et al.,<sup>22</sup> hepatic PMMR imaging showed a significantly shorter  $T_1$  value of the lateral segment of the left lobe, but no significant differences were noted in the anterior segment of the right lobe and  $T_2$  values of the both sites.

In the liver after death, decomposition and cooling<sup>24</sup> affects  $T_1$  and  $T_2$  values of MR imaging due to changes in the components and property of the liver, including fat, water, and paramagnetic substances such as iron,<sup>25</sup> all of which are expressed as relaxation time changes of the entire liver. In a living body, motion-induced imaging artifacts occur due to pulsatile blood flow; thus, deviations in the measurement of  $T_1$  and  $T_2$  values are normalized. However, with PMMRI,  $T_1$  and  $T_2$  values do not include such artifacts.

As decomposition occurs after death, the increase of phosphoric, carbonic, fatty, and lactic acids induces acidosis of the liver and reduces the pH.<sup>26,27</sup> Investigating the livers of rats, Moser et al. reported that reduction of the pH caused the prolongation of  $T_2$  values, though they did not mention  $T_1$  values.<sup>28</sup> We suggest that pH reduction in the postmortem human liver can cause the prolongation of  $T_2$  values.

The increased water content of tissues causes the elevation of  $T_1$  and  $T_2$  values,<sup>29</sup> although those of the liver are not the focus of attention in our study. Following death, the brain shows a time-course increase in water content due to the absorption of spinal fluid around the brain.<sup>30,31</sup> This is attributed to increased lactic acid as a result of anaerobic glycolysis and increased osmotic pressure due to an increased number of proteins caused by autolysis in the ischemic brain.<sup>32–34</sup> However, the liver in our study is considered not to have shown increased water content for a similar reason, because none of our cases exhibited ascites around the liver. An increase in the water content of the liver is known to sometimes occur with a prolonged agonal stage,<sup>35</sup> although this does not apply to our study since we investigated sudden death cases.

The Bloembergen-Purcell-Pound theory states that changes in  $T_1$  and  $T_2$  values are related to temperature change.<sup>36</sup> Therefore, the cooling of the body after death and subsequent storage of the cadaver in a refrigerator are considered to be the causes of MR relaxation time changes. Within a small temperature range, the  $T_1$  value depends linearly on the temperature in fat and water.<sup>14,15,37–41</sup> The  $T_2$  value decreases with a declining temperature in fat tissue and aqueous solutions;<sup>37,40,41</sup> however, the temperature dependence of the  $T_2$  value can be masked by other factors in tissue.<sup>37</sup>

The magnetic susceptibility of a paramagnetic substance is inversely proportional to the absolute temperature according to Curie's law (magnetic susceptibility  $\chi = C/T$ , where  $C$  is a constant and  $T$  is the absolute temperature).<sup>37</sup> The liver contains some paramagnetic substances such as iron, manganese, and copper.<sup>42–44</sup>

The increased magnetic susceptibility associated with temperature reduction induces changes in the relaxation time and has a very weak  $T_1$ -shortening effect but strong  $T_2$ -shortening effect.<sup>45</sup>

In the liver of our PMMR imaging,  $T_1$  values were shorter than the reported clinical MR imaging<sup>22</sup> in the lateral segment of the left lobe, but not much difference was found in the anterior segment of the right lobe. This  $T_1$ -shortening effect is due to the effect of fat and water at low temperatures. However,  $T_1$  values on hepatic PMMR imaging did not correlate significantly with the rectal temperature. Matsumoto et al.<sup>38</sup> reported that the  $T_1$  value of a pig liver *in vitro* decreased linearly with a temperature reduction range of 10–50°C, although the  $T_1$  value increased between the range of 0–10°C. Moser et al.<sup>28</sup> reported that in a temperature below 37°C, at 4 hours after biopsy excision,  $T_1$  values were higher in a rat liver *in vitro* at 22, 15, 30, 7, and 37°C, in this order. Namely,  $T_1$  value reduction was not proportional to the temperature reduction. In our study, the  $T_1$  value of the postmortem liver varied at low temperature over a similar range, which is considered to be the reason for not showing linearity regarding the relationship between the  $T_1$  value and rectal temperature.

Regarding  $T_2$  values, compared with clinical MR imaging of the liver, hepatic PMMR imaging did not show any significant change. For the liver,  $T_2$  prolongation due to a reduced pH,  $T_2$  shortening due to fat, water, and paramagnetic substances at low temperature negated each other. However,  $T_2$  values on hepatic PMMR imaging were correlated significantly with the rectal temperature. Also, according to Moser et al., at 4 hours after biopsy excision in a temperature below 37°C, high  $T_2$  values of a rat liver *in vitro* were observed at 37, 30, 22, 15, and 7°C in this decreasing order, showing the proportional reduction of  $T_2$  values relative to the temperature. In our study, the relationship between  $T_2$  value and rectal temperature of the liver showed linearity.

With hepatic PMMR imaging,  $T_1$  values did not correlate significantly with the rectal temperature, but  $T_2$  values significantly correlated. On the other hand, with cerebral PMMR imaging, it has been known that  $T_1$  values correlates significantly with rectal temperature, though  $T_2$  values did not.<sup>13</sup> This discrepancy between hepatic and cerebral PMMR imaging suggests organ-specific MR relaxation times after death.

Our study has four limitations. One is that we could not examine 1.5T MR imaging data of healthy volunteers, because an approximately 2-minute breath hold is necessary to obtain comparative imaging data.  $T_1$  and  $T_2$  values depend on the type of MR imaging unit and scan conditions; thus may differ on different imaging units or with different parameters.<sup>23</sup> In our study, we had to compare hepatic PMMR imaging data we gener-

ated with published data from clinical MR imaging of the liver in the literature. The second limitation is that the standard deviation of  $T_1$  value of our subjects were large compared to that of living subjects as reported by de Bazelaire et al.<sup>22</sup> Decomposition of the liver progresses in cases in which a long period of time elapsed after death. In our study, PMMR imaging was performed 7–96 hours after the confirmation of death. Our subjects had been kept in cold storage, which reduces decomposition of the body. Nevertheless, the wide deviation in the time after death may have caused differences of the degree of decomposition in each body, thereby resulting in increased standard deviation values. Also, a possible uneven rate of decomposition within the liver of a deceased subject may cause a difference in  $T_1$  shortening effects between the right anterior and left lateral segments of the liver. The third limitation is that  $B_1$  inhomogeneity correction was not performed with our relaxation time map creation tool, which is considered to have resulted in regional signal variation. A greater variation can be induced in the  $T_1$  map which is based on gradient echo sequences than the  $T_2$  map which is based on spin echo sequences. The fourth limitation is that we did not directly measure the pH, fat, water, and paramagnetic substances. Such measurement with an MR imaging system<sup>46–48</sup> would enable estimation of the level of effect of relaxation time changes of each factor on the total liver relaxation time.

## Conclusion

In conclusion, with hepatic PMMR imaging,  $T_1$  values did not significantly correlate with the rectal temperature, but  $T_2$  values did correlate. Postmortem interval had no effect on  $T_1$  and  $T_2$  values on hepatic PMMR imaging. Reduction in body temperature after death is considered to induce  $T_1$  and  $T_2$  value changes on hepatic PMMR imaging.

## Acknowledgement

This work was supported by a grant from the Daiwa Securities Health Foundation. The authors thank Ms. Yumiko Moriyama for her help with manuscript preparation.

The study was presented at the 21th annual meeting of the SMRT (Section for Magnetic Resonance Technologists), May 5-6, 2012, Melbourne, Australia.

## References

1. Brogdon BG. Research and applications of the new modalities. In: Brogdon BG, ed. *Forensic Radiology*, 1st ed. Boca Raton: CBC, 1998; 333–338.
2. Swift B, Ruttly GN. Recent advances in postmortem forensic radiology computed tomography and magnetic resonance imaging applications. In: Tsokos M, ed. *Forensic Pathology Reviews*, 1st ed. Totowa: Humana, 2006; 355–404.
3. Oesterhelweg L, Thali MJ. Experiences with virtual autopsy approach worldwide. In: Thali MJ, Dirnhofer R, Vock P, eds. *The Virtopsy Approach*, 1st ed. Boca Raton: CRC, 2009; 475–477.
4. Takahashi N, Higuchi T, Shiotani M, et al. The effectiveness of postmortem multidetector computed tomography in the detection of fatal findings related to cause of non-traumatic death in the emergency department. *Eur Radiol* 2012; 22:152–160.
5. Okuda T, Shiotani S, Sakamoto N, Kobayashi T. Background and current status of postmortem imaging in Japan: short history of “Autopsy imaging (Ai).” *Forensic Sci Int* 2013; 225:3–8.
6. Ruttly GN, Brogdon G, Dedouit F, et al. Terminology used in publications for post-mortem cross-sectional imaging. *Int J Legal Med* 2013; 127:465–466.
7. Mogan B, Adlam D, Robinson C, Pakkal M, Ruttly GN. Adult post-mortem imaging in traumatic and cardiorespiratory death and its relation to clinical radiological imaging. *Br J Radiol* 2014; 87:20130662.
8. Otake Y, Handa S, Kose K, Shiota K, Yamada S, Uwabe C. Magnetic resonance microscopy of chemically fixed human embryos at high spatial resolution. *Magn Reson Med Sci* 2015; 14:153–158.
9. Ruder TD, Thali MJ, Hatch GM. Essentials of forensic post-mortem MR imaging in adults. *Br J Radiol* 2014; 87:20130567.
10. Kobayashi T, Shiotani S, Kaga K, et al. Characteristic signal intensity changes on postmortem magnetic resonance imaging of the brain. *Jpn J Radiol* 2010; 28:8–14.
11. Kobayashi T, Isobe T, Shiotani S, et al. Postmortem magnetic resonance imaging dealing with low temperature objects. *Magn Reson Med Sci* 2010; 9:101–108.
12. Ruder TD, Hatch GM, Siegenthaler L, et al. The influence of body temperature on image contrast in post mortem MRI. *Eur J Radiol* 2012; 81:1366–1370.
13. Tashiro K, Shiotani S, Kobayashi T, et al. Cerebral relaxation times from postmortem MR imaging of adults. *Magn Reson Med Sci* 2014; 14:51–56.
14. Kobayashi T, Monma M, Baba T, et al. Optimization of inversion time for postmortem short-tau inversion recovery (STIR) MR imaging. *Magn Reson Med Sci* 2014; 13:67–72.
15. Abe K, Kobayashi T, Shiotani S, et al. Optimization of inversion time for postmortem fluid-attenuated inversion recovery (FLAIR) MR imaging at 1.5 T: Temperature-based suppression of cerebrospinal fluid. *Magn Reson Med Sci* 2015; 14:251–255.
16. Zech WD, Schwendener N, Persson A, Warntjes MJ, Jackowski C. Temperature dependence of postmortem MR quantification for soft tissue discrimination. *Eur Radiol* 2015; 25:2381–2389.
17. Lewa CJ, Majewska Z. Temperature relationships of proton spin-lattice relaxation time  $T_1$  in biological tissues. *Bull Cancer* 1980; 67:525–530.

18. Bottomley PA, Foster TH, Argersinger RE, Pfeifer LM. A review of normal tissue hydrogen NMR relaxation times and relaxation mechanisms from 1–100 MHz: dependence on tissue type, NMR frequency, temperature. *Med Phys* 1984; 11:425–448.
19. de Certaines JD, Henriksen O, Spisni A, Cortsen M, Ring PB. *In vivo* measurements of proton relaxation times in human brain, liver, and skeletal muscle: a multicenter MRI study. *Magn Reson Imaging* 1993; 11:841–850.
20. Blüml S, Schad LR, Stepanow B, Lorenz WJ. Spin-lattice relaxation time measurement by means of a Turbo FLASH technique. *Magn Reson Med* 1993; 30:289–295.
21. Akber SF. NMR relaxation data of water proton in normal tissues. *Physiol Chem Phys Med NMR* 1996; 28:205–238.
22. de Bazelaire CM, Duhamel GD, Rofsky NM, Alsop DC. MR imaging relaxation times of abdominal and pelvic tissues measured *in vivo* at 3.0 T: preliminary results. *Radiology* 2004; 230:652–659.
23. Kobayashi T, Ookubo J, Monma M, et al. [Evaluation of measurement accuracy of a T<sub>1</sub> and T<sub>2</sub> mapping tool]. *Jpn J Magn Reson Med* 2012; 32:66–75. (Article in Japanese with English abstract)
24. Saukko P, Knight B. The pathophysiology of death. In: Saukko P, Knight B, eds. *Knight's Forensic Pathology*, 3rd ed. London: Edward Arnold, 2004; 52–97.
25. Sharma P, Altbach M, Galons JP, Kalb B, Martin DR. Measurement of liver fat fraction and iron with MRI and MR spectroscopy techniques. *Diagn Interv Radiol* 2014; 20:17–26.
26. Sevringhaus EL. Postmortem acidity. 1. The acids formed in autolyzing liver. *J Biological Chem* 1923; 57:181–189.
27. Sevringhaus EL. Postmortem acidity. II. Phosphoric acid liberation in liver autolysis. *J Biological Chem* 1923; 57:191–197.
28. Moser E, Winklmayr E, Holzmüller P, Krssak M. Temperature- and pH-dependence of proton relaxation rate in rat liver tissue. *Magn Reson Imaging* 1995; 13:429–440.
29. Kiricuta IC Jr, Simplăceanu V. Tissue water content and nuclear magnetic resonance in normal and tumor tissues. *Cancer Res* 1975; 35:1164–1167.
30. Takahashi K. Relationship between acidity and swelling in the brain. *Tohoku J Exp Med* 1966; 90:261–268.
31. Katayama Y, Terashi A, Nagadumi A, et al. Studies on production of cerebral edema in complete ischemia. *Myakukangaku (Angiology)* 1984; 24:1271–1274. (Article in Japanese)
32. Myers RE, Yamaguchi M. Effect of serum glucose concentration on brain response to circulatory arrest. *J Neuropathol Exp Neurol* 1976; 35:301.
33. Yamaguchi M, Myers RE. Comparison of brain biochemical changes produced by anoxia and hypoxia. *J Neuropathol Exp Neurol* 1976; 35:302.
34. Bandaranayake NM, Nemoto EM, Stezoski SW. Rat brain osmolality during barbiturate anesthesia and global brain ischemia. *Stroke* 1978; 9:249–254.
35. Trowell OA. The experimental production of watery vacuolation of the liver. *J Physiol* 1946; 105:268–297.
36. Bloembergen N, Purcell EM, Pound RV. Relaxation effects in nuclear magnetic resonance absorption. *Physiol Rev* 1948; 73:679–712.
37. Rieke V, Butts Pauly K. MR thermometry. *J Magn Reson Imaging* 2008; 27:376–390.
38. Matsumoto R, Oshio K, Jolesz FA. Monitoring of laser and freezing-induced ablation in the liver with T1-weighted MR imaging. *J Magn Reson Imaging* 1992; 2:555–562.
39. Hynynen K, McDannold N, Mulkern RV, Jolesz FA. Temperature monitoring in fat with MRI. *Magn Reson Med* 2000; 43:901–904.
40. Gandhi S, Daniel BL, Butts K. Temperature dependence of relaxation times in bovine adipose tissue. *Proc Soc Magn Reson Med* 1998; 701–750.
41. Kuroda K, Iwabuchi T, Obara M, Honda M, Saito K, Imai Y. Temperature dependence of relaxation times in proton components of fatty acids. *Magn Reson Med Sci* 2011; 10:177–183.
42. Schumacher JH, Matys ER, Clorius JH, Hauser H, Wesch H, Maier-Borst W. Contribution of paramagnetic trace elements to the spin-lattice relaxation time in the liver. *Invest Radiol* 1985; 20:601–608.
43. Ling GN, Kolebic T, Damadian R. Low paramagnetic content in cancer cells: its significance in cancer detection by magnetic resonance imaging. *Physiol Chem Phys Med NMR* 1990; 22:1–14.
44. Honda H, Kaneko K, Kanazawa Y, et al. MR imaging of hepatocellular carcinomas: effect of Cu and Fe contents on signal intensity. *Abdom Imaging* 1997; 2:60–66.
45. Gossuin Y, Roch A, Muller RN, Gillis P. Relaxation induced by ferritin and ferritin-like magnetic particles: the role of proton exchange. *Magn Reson Med* 2000; 43:237–243.
46. van Zijl P, Yadav N. Chemical exchange saturation transfer (CEST): what is in a name and what isn't? *Magn Reson Med* 2011; 65:927–948.
47. Qayyum A. MR spectroscopy of the liver: principles and clinical applications. *Radiographics* 2009; 29:1653–1664.
48. Gandon Y, Olivie D, Guyader D, et al. Non-invasive assessment of hepatic iron stores by MRI. *Lancet* 2004; 363:357–362.